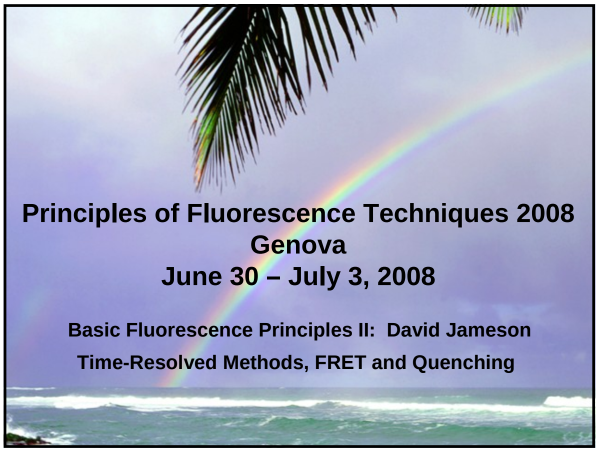

What is meant by the "lifetime" of a fluorophore???

Although we often speak of the properties of fluorophores as if they are studied in isolation, such is not usually the case.

Absorption and emission processes are almost always studied on *populations* of molecules and the properties of the supposed typical members of the population are deduced from the macroscopic properties of the process.

In general, the behavior of an excited population of fluorophores is described by a familiar rate equation:

$$\frac{dn^*}{dt} = -n^* \Gamma + f(t)$$

where n^* is the number of excited elements at time t, Γ is the rate constant of emission and f(t) is an arbitrary function of the time, describing the time course of the excitation . The dimensions of Γ are sec^{-1} (transitions per molecule per unit time).

If excitation occurs at t = 0, the last equation, takes the form:

$$\frac{dn^*}{dt} = -n^* \Gamma$$

and describes the decrease in excited molecules at all further times. Integration gives:

$$n^*(t) = n^*(0) \exp(-\Gamma t)$$

The lifetime, τ, is equal to Γ^{-1}

If a population of fluorophores are excited, the lifetime is the time it takes for the number of excited molecules to decay to 1/e or 36.8% of the original population according to:

$$\frac{n^*(t)}{n^*(0)} = e^{-t/\tau}$$

In pictorial form:

$$\frac{n^*(t)}{n^*(0)} = e^{-t/\tau}$$

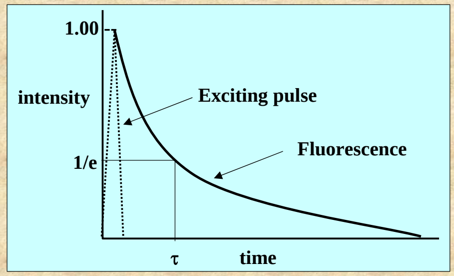

Knowledge of a fluorophore's excited state lifetime is crucial for quantitative interpretations of numerous fluorescence measurements such as quenching, polarization and FRET.

In most cases of interest, it is virtually impossible to predict *a priori* the excited state lifetime of a fluorescent molecule. The true molecular lifetime, i.e., the lifetime one expects in the absence of any excited state deactivation processes – can be approximated by the Strickler-Berg equation (1962, J. Chem. Phys. 37:814).

$$\tau_m^{-1} = 2.88\text{x}10^{-9} n^2 \langle \nu_f^{-3} \rangle \int_{\Delta\nu_a} \varepsilon(\bar{\nu})\, d\ln\bar{\nu}$$

where

$$\langle \nu_f^{-3} \rangle = \frac{\int_{\Delta\nu_e} F(\nu)\,d\nu}{\int_{\Delta\nu_a} F(\nu)\nu^{-3}\,d\nu}$$

τ_m is the molecular lifetime, n is the refractive index of the solvent, $\Delta\nu_e$ and $\Delta\nu_a$ correspond to the experimental limits of the absorption and emission bands (S_0 - S_1 transitions), ε is the molar absorption and $F(\nu)$ describes the spectral distribution of the emission in photons per wavelength interval.

How well do these equations actually work?

Not very well – sometimes off by factors of 2 – 5 fold.

The lifetime and quantum yield for a given fluorophore are often dramatically affected by its environment.

Examples of this fact would be NADH, which in water has a lifetime of ~0.4 ns but bound to dehydrogenases can be a long as 9 ns.

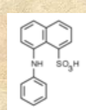

ANS in water is ~100 picoseconds but can be 8 – 10 ns bound to proteins

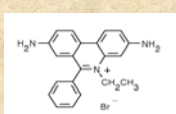

Ethidium bromide is 1.8 ns in water, 22 ns bound to DNA and 27ns bound to tRNA

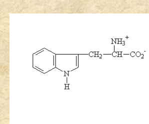

The lifetime of tryptophan in proteins ranges from ~0.1 ns up to ~8 ns

Excited state lifetimes have traditionally been measured using either the *impulse* response or the *harmonic* response method. In principle both methods have the same information content. These methods are also referred to as either the “time domain” method or the “frequency domain” method.

In the *impulse (*or pulse) method, the sample is illuminated with a short pulse of light and the intensity of the emission versus time is recorded. Originally these short light pulses were generated using *flashlamps* which had widths on the order of several nanoseconds. Modern laser sources can now routinely generate pulses with widths on the order of picoseconds or shorter.

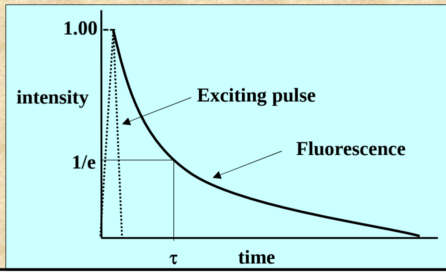

As shown in the intensity decay figure, the *fluorescence* lifetime, τ , is the time at which the intensity has decayed to 1/e of the original value. The decay of the intensity with time is given by the relation:

$$I_t = \alpha e^{-t/\tau}$$

Where I_t is the intensity at time t, α is a normalization term (the pre-exponential factor) and τ is the lifetime.

It is more common to plot the fluorescence decay data using a logarithmic scale as shown here.

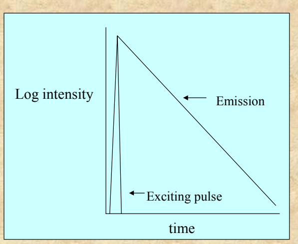

If the decay is a single exponential and if the lifetime is long compared to the exciting light then the lifetime can be determined directly from the slope of the curve.

If the lifetime and the excitation pulse width are comparable some type of *deconvolution* method must be used to extract the lifetime.

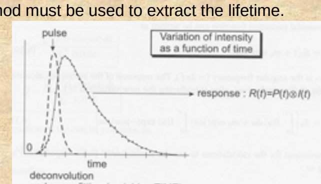

Great effort has been expended on developing mathematical methods to “deconvolve” the effect of the exciting pulse shape on the observed fluorescence decay.

With the advent of very fast laser pulses these deconvolution procedures became less important for most lifetime determinations, although they are still required whenever the lifetime is of comparable duration to the light pulse.

If the decay is multiexponential, the relation between the intensity and time after excitation is given by:

$$I(t) = \sum_i \alpha_i e^{-t/\tau_i}$$

One may then observe data such as those sketched below:

Here we can discern at least two lifetime components indicated as τ_1 and τ_2. This presentation is oversimplified but illustrates the point.

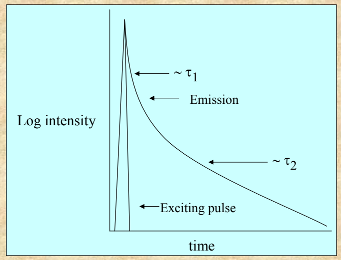

Here are pulse decay data on anthracene in cyclohexane taken on an IBH 5000U Time-correlated single photon counting instrument equipped with an LED short pulse diode excitation source.

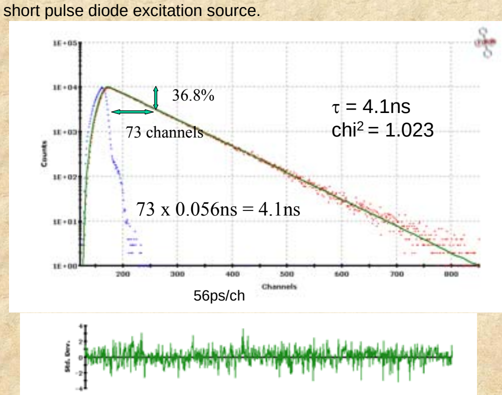

In the harmonic method (also known as the phase and modulation or frequency domain method) a continuous light source is utilized, such as a laser or xenon arc, and the intensity of this light source is modulated sinusoidally at high frequency as depicted below. Typically, an *electro-optic* device, such as a *Pockels cell* is used to modulate a continuous light source, such as a CW laser or a xenon arc lamp. Alternatively, LEDs or laser diodes can be directly modulated.

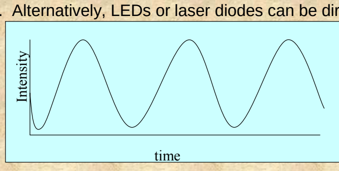

In such a case, the excitation frequency is described by:

$$E(t) = Eo\,[1 + M_E \sin \omega t]$$

E(t) and Eo are the intensities at time t and o, M_E is the modulation factor which is related to the ratio of the AC and DC parts of the signal and ω is the angular modulation frequency.

$\omega = 2\pi f$ where f is the linear modulation frequency

Due to the persistence of the excited state, fluorophores subjected to such an excitation will give rise to a modulated emission which is shifted in phase relative to the exciting light as depicted below.

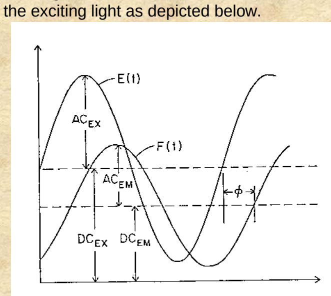

This sketch illustrates the phase delay (ϕ) between the excitation, E(t), and the emission, F(t). Also shown are the AC and DC levels associated with the excitation and emission waveforms.

One can demonstrate that:

$$\mathbf{F(t) = Fo\,[1 + M_F \sin(\omega t + \phi)]}$$

This relationship signifies that measurement of the phase delay, ϕ, forms the basis of one measurement of the lifetime, τ. In particular one can demonstrate that:

$$\mathbf{\tan\phi = \omega\tau}$$

The *modulations* of the excitation (M_E) and the emission (M_F) are given by:

$$M_E = \left(\frac{AC}{DC}\right)_E \quad \text{and} \quad M_F = \left(\frac{AC}{DC}\right)_F$$

The *relative modulation*, M, of the emission is then:

$$M = \frac{(AC/DC)_F}{(AC/DC)_E}$$

τ can also be determined from M according to the relation: $M = \dfrac{1}{\sqrt{1+(\omega\tau)^2}}$

Using the *phase shift* and *relative modulation* one can thus determine a *phase lifetime* (τ_P) and a *modulation lifetime* (τ_M).

If the fluorescence decay is a single exponential, then τ_P and τ_M will be equal at all modulation frequencies.

If, however, the fluorescence decay is multiexponential then $\tau_P < \tau_M$ and, moreover, the values of both τ_P and τ_M will depend upon the modulation frequency, i.e.,

$$\boldsymbol{\tau_P(\omega_1) < \tau_P(\omega_2) \quad \text{if} \quad \omega_1 > \omega_2}$$

To get a feeling for typical phase and modulation data, consider the following data set.

Frequency (MHz)	τ_P (ns)	τ_M (ns)
5	6.76	10.24
10	6.02	9.70
30	3.17	6.87
70	1.93	4.27

These differences between τ_P and τ_M and their frequency dependence form the basis of the methods used to analyze for lifetime heterogeneity, i.e., the component lifetimes and amplitudes.

In the case just shown, the actual system being measured was a mixture of two fluorophores with lifetimes of 12.08 ns and 1.38 ns, with relative contributions to the total intensity of 53% and 47% respectively.

Here must must be careful to distinguish the term *fractional contribution to the total intensity* (usually designated as f) from α, the pre-exponential term referred to earlier. The relation between these two terms is given by:

$$f_i = \frac{\alpha_i \tau_i}{\sum_j \alpha_j \tau_j}$$

where j represents the sum of all components. In the case just given then, the ratio of the pre-exponential factors corresponding to the 12.08 ns and 1.38 ns components is approximately 1/3. In other words, there are three times as many molecules in solution with the 1.38 ns lifetime as there are molecules with the 12.08 ns lifetime.

Multifrequency phase and modulation data are usually presented as shown below:

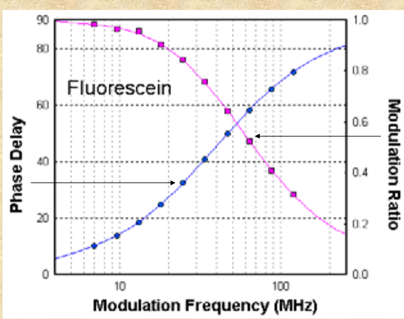

The plot shows the frequency response curve (phase and modulation) of Fluorescein in phosphate buffer pH 7.4 acquired on an ISS Chronos using a 470 nm LED. The emission was collected through a 530 high pass filter. The data is best fitted by a single exponential decay time of 4 ns.

A case of multi-exponential decays is shown here for a system of two lifetime species of 8.7ns and 3.1ns and a 1 to 1 mixture (in terms of fractional intenisties)

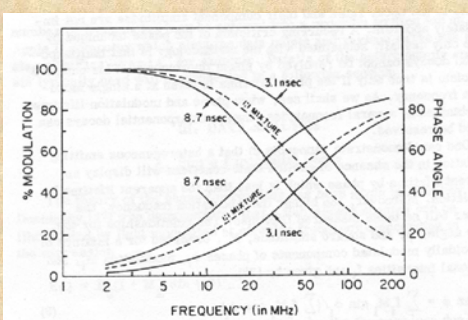

Multifrequency phase and modulation data is usually analyzed using a non-linear least squares method in which the actual phase and modulation ratio data (<u>not</u> the lifetime values) are fit to different models such as single or double exponential decays.

The quality of the fit is then judged by the *chi-square value* (χ^2) which is given by:

$$\chi^2 = \{[(Pc - Pm)/\sigma^P] + (Mc - Mm)/\sigma^M]\}/(2n - f - 1)$$

where P and M refer to phase and modulation data, respectively, c and m refer to calculated and measured values and σ^P and σ^M refer to the standard deviations of each phase and modulation measurement, respectively. n is the number of modulation frequencies and f is the number of free parameters.

In addition to decay analysis using discrete exponential decay models, one may also choose to fit the data to *distribution* models. In this case, it is assumed that the excited state decay characteristics of the emitting species actually results in a large number of lifetime components. Shown below is a typical lifetime distribution plot for the case of single tryptophan containing protein – human serum albumin.

The distribution shown here is Lorentzian but depending on the system different types of distributions, e.g., Gaussian or asymmetric distributions, may be utilized. This approach to lifetime analysis is described in: Alcala, J. R., E. Gratton and F. G. Prendergast. Fluorescence lifetime distributions in proteins. *Biophys. J. 51*, 597-604 (1987).

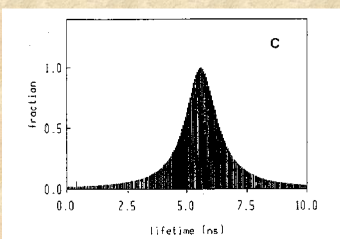

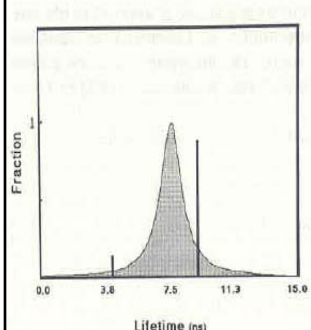

FIGURE 4. Continuous distribution (Lorentzian) lifetime analysis for methylanthraniloyl-GDP bound to the N-ras, P21 protein product (20°C). Calculated lifetime and full width at half-maximum were 7.7 and 1.1 nsec, respectively. The vertical dotted lines represent a two-component discrete lifetime fit to the same data: τ_1 = 8.5 nsec, 86% of the intensity, and τ_2 = 3.9 nsec. The χ^2 values were similar in both cases.

Another popular lifetime analysis method – based on Information Theory - is the *Maximum Entropy Method* (MEM). In this method no *a priori* intensity decay model is assumed.

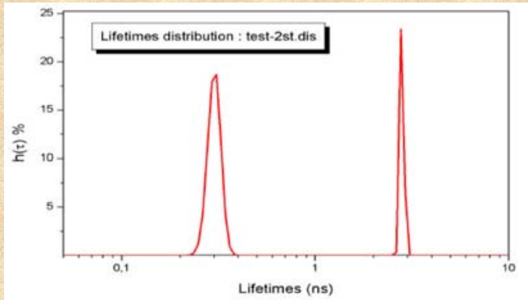

Jean-Claude Brochon
Maximum entropy method of data analysis in time-resolved spectroscopy.
Methods Enzymol. 1994;240:262-311.

Wavelength dependent lifetime data can be used to resolve individual spectra in a mixture

Gratton, E. and Jameson, D.M. (1985) *Anal. Chem. 57*:1694-1697. New Approach to Phase and Modulation Resolved Spectra.

Mixture: Lifetimes were 10.8ns, 4.3ns and 0.9ns

Spectra of individual components

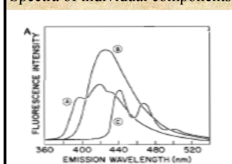

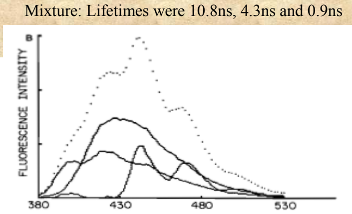

Figure 3. (A) Intensity spectra of individual components, POPOP (A), DENS (B), and perylene (C) in ethanol (not degassed). (B) Intensity (dotted line) and phase resolved spectra (solid lines) for the ternary mixture in A.

Global Analysis

In Global Analysis one can link decay parameters across many data sets which often allows for a more robust analysis

Example of the application of Global Analysis

Binding of Ethidium-Bromide to Transfer RNA

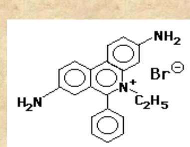

Ethidium Bromide

Yeast phenylalanine tRNA

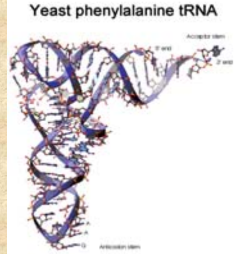

Ethidium bromide can intercalate into nucleic acid structures
It binds well to both DNA and RNA

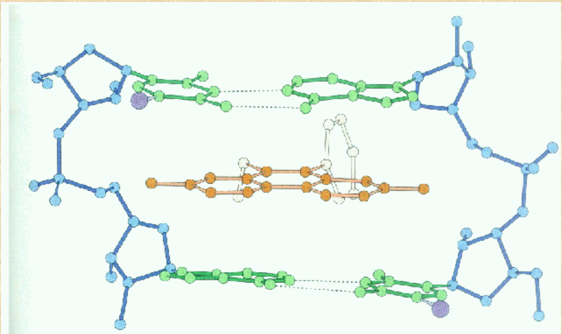

Fluorescence investigations of EB - tRNA interactions, carried out for more than 30 years, have indicated a "strong" binding site and one or more "weak, non-specific" binding sites.

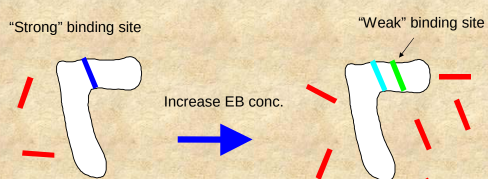

Question: What are the lifetimes of the strong and the weak binding sites???

If the tRNA is in excess only one EB will bind to the "strong" binding site which has a K_d of around 1 micromolar (under these conditions a single exponential decay of 27ns is observed). If the EB/tRNA ratio is increased, one or more additional EB's will bind and the question is: What are the lifetimes of EB bound to different sites on tRNA?" Shown below are phase and modulation data for a solution containing 124 μM yeast $tRNA^{phe}$ and 480 μM EB

The phase and modulation data were first fit to a single exponential component shown as the solid lines in the top plot. The residuals for this fit are shown in the bottom plot.

In this case τ = 18.49 ns and the χ^2 value was 250.

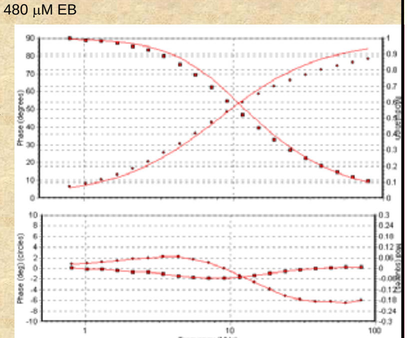

The data were then fit to a 2-component model shown here In this case the two lifetime components were 22.71 ns with a fractional intensity of 0.911 and 3.99 ns with a fractional intensity of 0.089.

The χ^2 for this fit was 3.06 (note the change in scale for the residual plot compared to the first case shown).

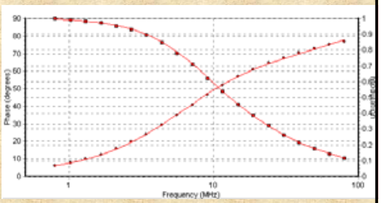

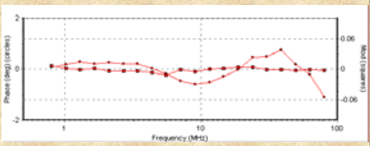

A 3-component model improves the fit still more. In this case

τ_1 = 24.25 ns, f_1 = 0.83

τ_2 = 8.79 ns, f_2 = 0.14

τ_3 = 2.09 ns, f_3 = 0.03

χ^2 = 0.39.

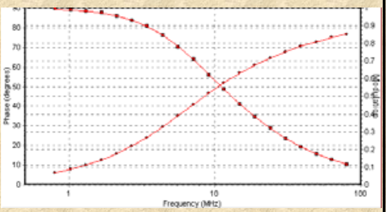

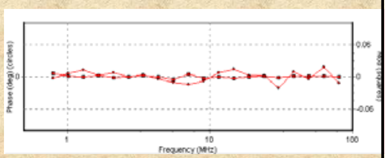

Adding a fourth component – with all parameters free to vary - does not lead to a significant improvement in the χ^2. In this case one finds 4 components of 24.80 ns (0.776), 12.13ns (0.163), 4.17 ns (0.53) and 0.88 ns (0.008).

But we are not using all of our information! We can actually fix some of the components in this case. We know that **free EB** has a lifetime of **1.84 ns** and we also know that the lifetime of **EB bound to the "strong" tRNA binding site** is **27 ns**. So we can fix these in the analysis. The results are four lifetime components of 27 ns (0.612), 18.33 ns (0.311), 5.85 ns (0.061) and 1.84 ns (0.016). The χ^2 improves to 0.16.

We can then go one step better and carry out **"Global Analysis"**.
In Global Analysis, multiple data sets are analyzed simultaneously and different parameters (such as lifetimes) can be "linked" across the data sets. The important concept in this particular experiment is that the lifetimes of the components stay the same and only their fractional contributions change as more ethidioum bromide binds.

In this system, 8 data sets, with increasing EB/tRNA ratios, were analyzed. Some of the data are shown below for EB/tRNA ratios of 0.27 (circles), 1.34 (squares), 2.41 (triangles) and 4.05 (inverted triangles).

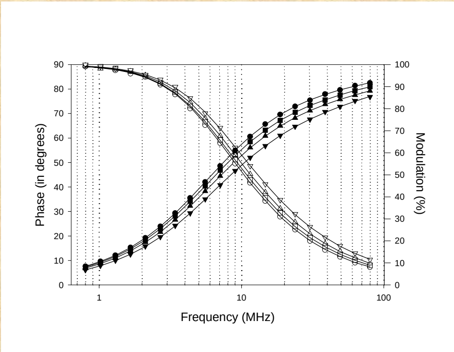

Global Analysis on seven data sets fit best to the 4 component model with two fixed components of 27ns and 1.84ns and two other components of 17.7ns and 5.4ns.

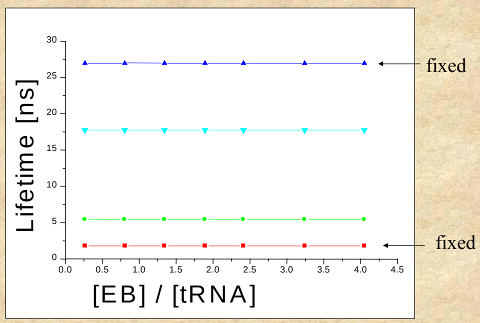

As shown in the plot below, as the EB/tRNA ratio increases the fractional contribution of the 27ns component decreases while the fractional contributions of the 17.7ns and 5.4ns components increase.

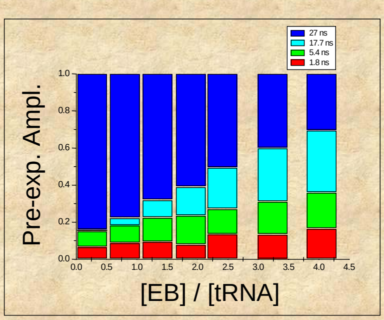

The Model

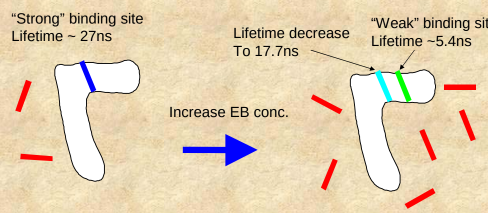

Question:
Is the drop in the lifetime of the "strong" binding site due to a change in tRNA conformation or energy transfer???

Answer: ???

Time-Resolved Anisotropy and Excited State Reactions

Many of these slides were prepared by Theodore Hazlett

Time-resolved methodologies provide information on the changes of orientation as a function of time of a system. The time-domain approach is usually termed the **anisotropy decay** method while the frequency-domain approach is known as **dynamic polarization**. In principle both methods yield the same information.

In the time-domain anisotropy method the sample is illuminated by a pulse of vertically polarized light and the decay over time of both the vertical and horizontal components of the emission are recorded. The anisotropy function is then plotted versus time as illustrated here:

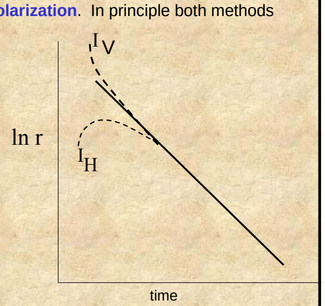

Note that the horizontal component actually increases during short times, since initially the fluorophores have not rotated significantly. As time passes though the number of horizontally oriented molecules increases

Simplest Case: Spherical Body

Fully Symmetrical

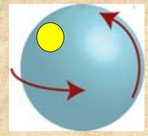

(in this case we assume that the fluorophore has no local mobility – such is the case for non-covalent interactions)

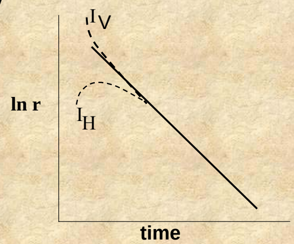

The decay of the anisotropy with time, r(t), for a sphere is given by:

$$r = \frac{Iv - Ih}{Iv + 2Ih} = r_o e^{-(t/\tau_c)}$$

τ_c is the rotational correlation time

$$\tau_c = \frac{1}{6 \cdot D_{rotation}}$$

In the case of non-spherical particles the time-decay of anisotropy function is more complicated. Mathematically simple symmetrical ellipsoids give us a sense of how changes in Shape affect the rotational diffusion rates.

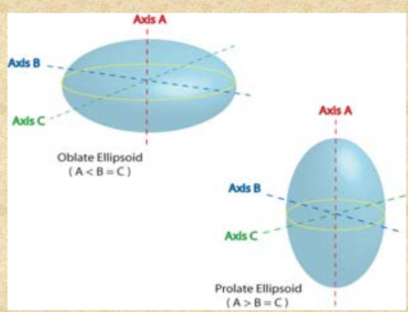

The Effect of Shape on Diffusion

Translational Diffusion

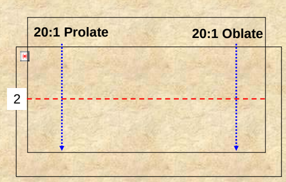

Rotational Diffusion

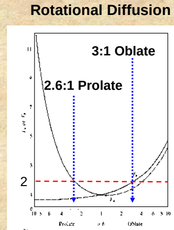

Rotational Diffusion is much more influenced by macromolecular shape

How are these Shapes Modeled?

In the case of symmetrical ellipsoids of revolution the relevant expression is:

$$r(t) = r_1 e^{\left(\frac{-t}{\tau_{c1}}\right)} + r_2 e^{\left(\frac{-t}{\tau_{c2}}\right)} + r_3 e^{\left(\frac{-t}{\tau_{c3}}\right)}$$

where: $\tau_{c1} = 1/6D_2$

$\tau_{c2} = 1/(5D_2 + D_1)$

$\tau_{c3} = 1/(2D_2 + 4D_1)$

D_1 and D_2 are the rotational diffusion coefficients about the axes of symmetry and about either equatorial axis, respectively.

Resolution of the rotational rates is limited in practice to two rotational correlation times which differ by at least a factor of two.

What do the Anisotropy Amplitudes (r1, r2, & r3) Represent?

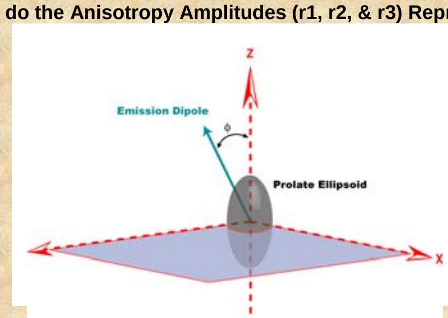

The amplitudes relate to orientation of the probe with respect to the axis of symmetry for the ellipsoid ***(we are assuming colinear excitation and emission dipoles).***

$r_1 = 0.1(3\cos^2\phi - 1)^2$
$r_2 = 0.3\sin^2(2\phi)$
$r_3 = 0.3\sin^4(\phi)$

Multiple Rotating Species (mixtures)

$$r(t) = r_1 e^{\left(\frac{-t}{\tau_{c1}}\right)} + r_2 e^{\left(\frac{-t}{\tau_{c2}}\right)}$$

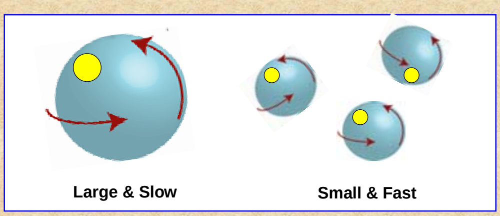

Mixed systems Show Simple, Multi-Exponential Behavior

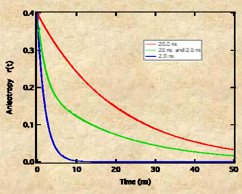

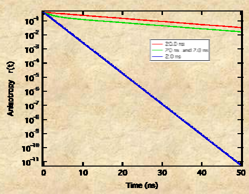

With separate species the decays reflect the sum of the exponential components present.

Multiple Rotational Modes: Local relaxation + Global rotation

Is the case of a **"local"** rotation of a probe attached to a spherical particle any different than multiple species?

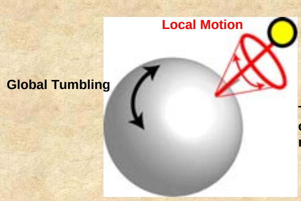

This common system represents a condition containing a hindered motion.

The expression for this case is:

$$r(t) = r_1 \cdot e^{-(t/\tau_{c1})} + r_2 \cdot e^{-(t/\tau_{c1} + t/\tau_{c2})}$$

Where τ_{c1} represents the "Global" probe motion, τ_{c2} represents the "Local" rotation of the macromolecule.

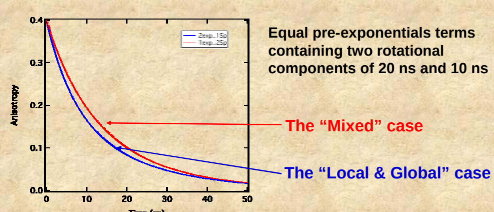

Equal pre-exponentials terms containing two rotational components of 20 ns and 10 ns

Hindered Rotational Systems
Membrane Bilayers

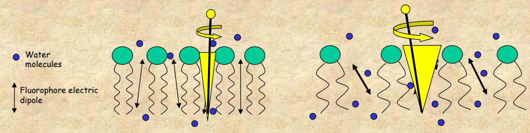

Wobble-in-a-Cone Concept

1) Freedom of motion
2) The rate of motion

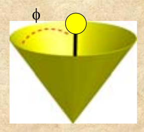

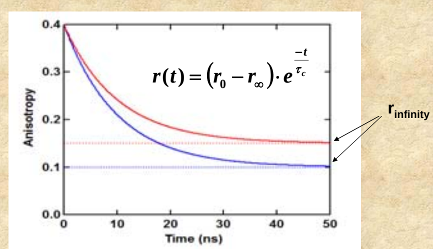

$$\frac{r_0}{r_\infty} = \left\langle \frac{3 \cdot \cos^2(\phi) - 1}{2} \right\rangle^2$$

Motion
τ_c = 20 ns

Angular Freedom
ϕ= 52 degrees
ϕ= 44 degrees

Analysis of Fluorophore Rotation in an Artificial Bilayer

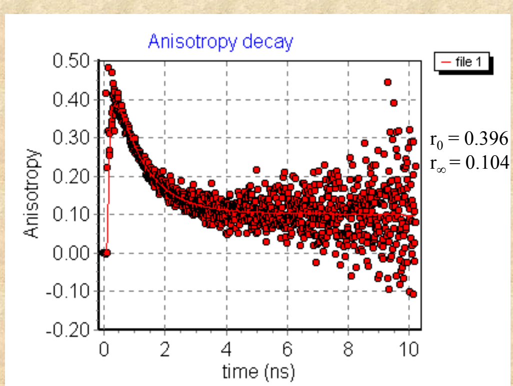

Phase & Modulation Measurements

In dynamic polarization measurements, the sample is illuminated with vertically polarized, modulated light. The phase delay (dephasing) between the parallel and perpendicular components of the emission is measured as well as the modulation ratio of the AC contributions of these components. The expressions a spherical particle are:

$$\Delta\phi = \tan^{-1}\left[\frac{18\omega r_o R}{(k^2+\omega^2)(1+r_o-2r_o^2)+6R(6R+2k+kr_o)}\right]$$

$$Y^2 = \frac{\left(((1-r_o)k+6R)^2+(1-r_o)^2\omega^2\right)}{[(1+2r_o)k+6R]^2+(1+2r_o)^2\omega^2}$$

Where $\Delta\phi$ is the phase difference, Y the modulation ratio of the AC components, ω the angular modulation frequency, r_o the limiting anisotropy, k the radiative rate constant ($1/\tau$) and R the rotational diffusion coefficient.

The illustration below depicts the $\Delta\phi$ function for the cases of spherical particles with different rotational relaxation times.

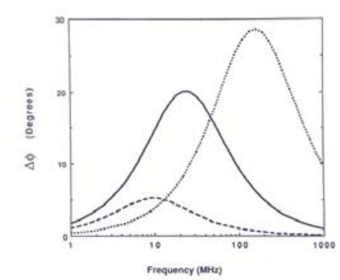

Differential phase data for an isotropic rotator with a 3-nsec (dotted line), 30-nsec (solid line), or 300-nsec (dashed line) rotational relaxation time. In each case a lifetime of 20 nsec was used and colinear excitation and emission dipoles were assumed.

The figures here show actual results for the case of ethidium bromide free and bound to tRNA - one notes that the fast rotational motion of the free ethidium results in a shift of the "bell-shaped" curve to higher frequencies relative to the bound case. The lifetimes of free and bound ethidium bromide were approximately 1.8 ns and 27 ns respectively.

126 David M. Jameson and Theodore L. Hazlett

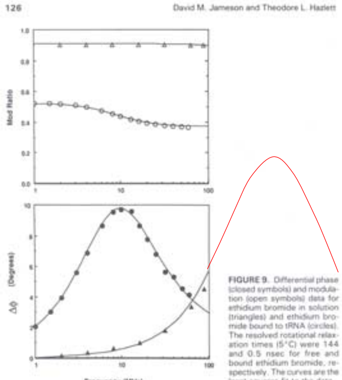

FIGURE 9. Differential phase (closed symbols) and modulation (open symbols) data for ethidium bromide in solution (triangles) and ethidium bromide bound to tRNA (circles). The resolved rotational relaxation times (5°C) were 144 and 0.5 nsec for free and bound ethidium bromide, respectively. The curves are the least-squares fit to the data.

In the case of local plus global motion, the dynamic polarization curves are altered as illustrated below for the case of the single tryptophan residue in elongation factor Tu which shows a dramatic increase in its local mobility when EF-Tu is complexed with EF-Ts.

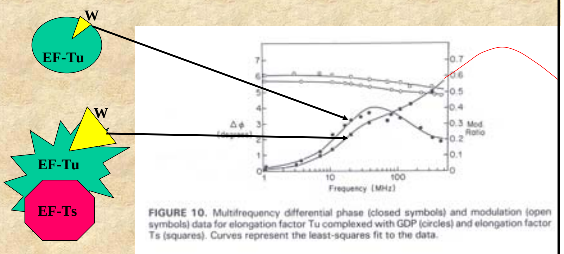

FIGURE 10. Multifrequency differential phase (closed symbols) and modulation (open symbols) data for elongation factor Tu complexed with GDP (circles) and elongation factor Ts (squares). Curves represent the least-squares fit to the data.

Final comment: Although we have discussed analysis of rotational rates in terms of discrete components, in some cases a more realistic approach may be to use distribution functions

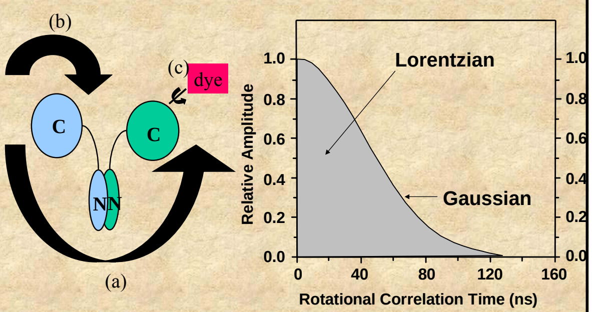

Förster Resonance Energy Transfer

FRET

Many of these slides were prepared by Pierre Moens

What is FRET ?

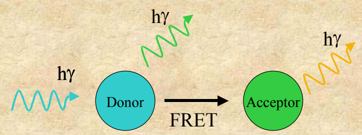

When the donor molecule absorbs a photon, and there is an acceptor molecule close to the donor molecule, radiationless energy transfer can occur from the donor to the acceptor.

FRET results in a decrease of the fluorescence intensity and lifetime of the donor probe, It enhance the fluorescence of the acceptor probe when the acceptor is fluorescent.

PM

FRET

Tuning fork analogy for resonance energy transfer

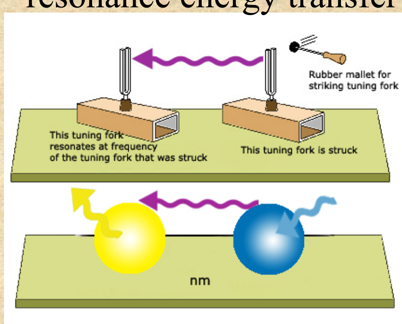

TV

Milestones in the Theory of Resonance Energy Transfer

1918 J. Perrin proposed the mechanism of resonance energy transfer

1922 G. Cario and J. Franck demonstrate that excitation of a mixture of mercury and thallium atomic vapors with 254nm (the mercury resonance line) also displayed thallium (sensitized) emission at 535nm.

1924 E. Gaviola and P. Pringsham observed that an increase in the concentration of fluorescein in viscous solvent was accompanied by a progressive depolarization of the emission.

1928 H. Kallmann and F. London developed the quantum theory of resonance energy transfer between various atoms in the gas phase. The dipole-dipole interaction and the parameter R_0 are used for the first time

1932 F. Perrin published a quantum mechanical theory of energy transfer between molecules of the same specie in solution. Qualitative discussion of the effect of the spectral overlap between the emission spectrum of the donor and the absorption spectrum of the acceptor

1946-1949 T. Förster develop the first quantitative theory of molecular resonance energy transfer

Simplified Energy Diagram

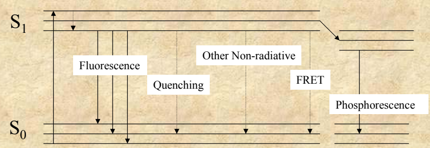

During the absorption process, the molecule is excited to one higher vibrational level of its first electronic excitation state. From there it is converted to lower vibrational levels of the same electronic state by reaching thermal equilibrium with its surrounding medium. Then, various processes can occur during the excited state lifetime of the fluorophore: radiative decays to the ground state by emission of a photon, inter-system crossing leading to phosphorescence and non-radiative decays such as dynamic quenching, photochemistry, charge transfer reactions and FRET.

Simplified FRET Energy Diagram

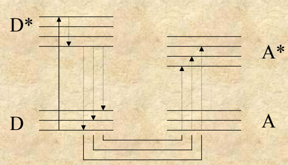

Coupled transitions

Suppose that the energy difference for one of these possible deactivation processes in the donor molecule matches that for a possible absorption transition in a nearby acceptor molecule. Then, with sufficient energetic coupling between these molecules (overlap of the emission spectrum of the donor and absorption spectrum of the acceptor), both processes may occur simultaneously, resulting in a transfer of excitation from the donor to the acceptor molecule

The interaction energy is of a dipole-dipole nature and depends on the distance between the molecules as well as the relative orientation of the dipoles

PM

Dipole-dipole interaction

The rate of transfer (k_T) of excitation energy is given by:

$$k_T = (1/\tau_d)(R_0/r)^6$$

Where τ_d is the fluorescence lifetime of the donor in the absence of acceptor, r the distance between the centers of the donor and acceptor molecules and R_0 the Förster critical distance at which 50% of the excitation energy is transferred to the acceptor and can be approximated from experiments independent of energy transfer.

Förster critical distance

$$R_0 = 0.2108\,(n^{-4} Q_d \kappa^2 J)^{1/6} \quad \text{Å}$$

- n is the refractive index of the medium in the wavelength range where spectral overlap is significant (usually between 1.2-1.4 for biological samples)
- Q_d is the fluorescence quantum yield of the donor in absence of acceptor (i.e. number of quanta emitted / number of quanta absorbed)
- κ^2 is the orientation factor for the dipole-dipole interaction
- J is the normalized spectral overlap integral [$\varepsilon(\lambda)$ is in $M^{-1}\,cm^{-1}$, λ is in nm and J are $M^{-1}\,cm^{-1}\,(nm)^4$]

The overlap integral J is defined by:

$$J = \int_0^\infty I_D(\lambda)\varepsilon_A(\lambda)\lambda^4 d\lambda$$

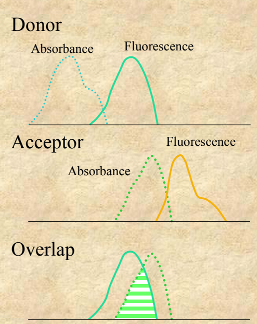

Where λ is the wavelength of the light, $\varepsilon_A(\lambda)$ is the molar absorption coefficient at that wavelength and $I_D(\lambda)$ is the fluorescence spectrum of the donor normalized on the wavelength scale:

$$I_D(\lambda) = \frac{F_{D\lambda}(\lambda)}{\int_0^\infty F_{D\lambda}(\lambda)d\lambda}$$

Where $F_{D\lambda}(\lambda)$ is the donor fluorescence per unit wavelength interval

The orientation factor κ^2

$$\kappa^2 = (\cos\theta_T - 3\cos\theta_D\cos\theta_A)^2$$

Where θ_T is the angle between the D and A moments, given by

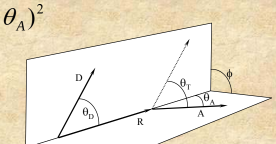

$$\cos\theta_T = \sin\theta_D\sin\theta_A\cos\phi + \cos\theta_D\cos\theta_A$$

In which θ_D, θ_A are the angles between the separation vector R, and the D and A moment, respectively, and ϕ is the azimuth between the planes (D,R) and (A,R)

The orientation factor κ^2

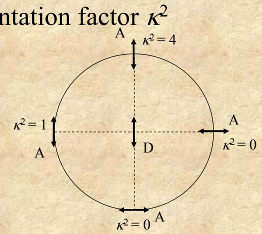

The limits for κ^2 are 0 to 4, The value of 4 is only obtained when both transitions moments are in line with the vector R. The value of 0 can be achieved in many different ways.

If the molecules undergo fast isotropic motions (dynamic averaging) then $\kappa^2 = 2/3$

From Eisinger and Dale in:"Excited States of Biological Molecules" Edited by John Birks (1976)

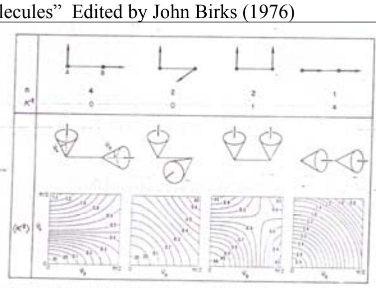

Figure 1 The upper part of the diagram illustrates the nine possible relative orientations of two transition dipoles each of which is fixed and can lie along either the x, y or z axis of a Cartesian triad. The corresponding κ^2 values are shown along with their statistical weights (n) and they are seen to lead to an average for κ^2 of 2/3, the same as for isotropically random orientations of the transition dipole moments. The lower part of the figure illustrates how these $\langle\kappa^2\rangle$ values change as the transition dipole directions are permitted orientational freedom within cones of half-angles ψ_A and ψ_B. Note that $\langle\kappa^2\rangle$ departs quite slowly from its fixed minimum and maximum values (0 and 4) as the two cones open up and that when each cone half-angle is $\pi/2$, corresponding to an isotropic distribution of the transition dipole directions, $\langle\kappa^2\rangle$ is equal to 2/3 for each of the cases considered

Determination of κ^2

Except in very rare case, κ^2 can not be uniquely determined in solution.
What value of κ^2 should be used ?

1. We can **assume** fast isotropic motions of the probes and a value of $\kappa^2 = 2/3$, and verify experimentally that it is indeed the case.

2. We can **calculate** the lower and upper limit of κ^2 using polarization spectroscopy (Dale, Eisinger and Blumberg 1979).

Assuming $\kappa^2 = 2/3$

We can verify this assumption experimentally by:

- Swapping probes
- Using different probes

***By swapping probes*:** The micro-environment of the probes will be different. Therefore, if the micro-environment affect the probes mobility and, κ^2 is not equal to 2/3, once swapped, the value of $\kappa 2$ will changed and hence the distance measured by FRET.

By using different probes: If the distance measured using different probe pairs are similar (taking into account the size of the probes) then the assumption that κ^2 is equal to 2/3 is probably valid.

Lower and upper limit of κ^2

2. We can **calculate** the lower and upper limit of κ^2 using polarization spectroscopy (Dale, Eisinger and Blumberg 1979).

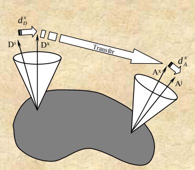

Lets consider that the each probe are rotating within a cone of axe D^x and A^x for the donor and acceptor, respectively, then 3 depolarization steps occurs after the absorption of the excitation energy by the donor: An axial depolarization of the donor, a depolarization due to transfer between the axes of the orientational distribution of the D and A and an axial depolarization of the acceptor

In the Dale-Eisinger-Blumberg approach, one measures the ratio of the observed polarizations of donors and acceptors to their limiting polarizations and then uses the calculated contour plots to put limits on κ^2

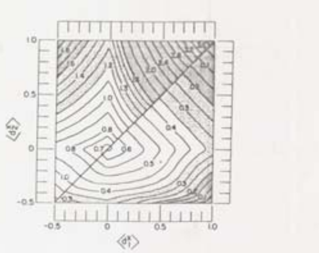

FIGURE 9 Contour plot similar to those shown in Figs. 4-8, but applicable in situations in which $\langle d_T \rangle$, and hence d_T^x, is unknown. It is obtained by maximizing and minimizing Eq. 21 and can be seen to lead to larger ranges between $\langle \kappa^2 \rangle_{min}$ and $\langle \kappa^2 \rangle_{max}$ than the plots of Figs. 4-8. In the heavily stippled regions the error in R resulting from the use of $\langle \kappa^2 \rangle = ⅔$ instead of the indicated $\langle \kappa^2 \rangle_{min}$ and $\langle \kappa^2 \rangle_{max}$ is greater than 20%. It is between 10% and 20% in the lightly stippled regions and less than 10% in the unstippled ones.

This approach was used in:
Arbildua et al.,
Fluorescence resonance energy transfer and molecular modeling studies on 4',6-diamidino-2-phenylindole (DAPI) complexes with tubulin.
Protein Sci. (2006) 15(3):410-9.

FRET occurs between DAPI and TNP-GTP bound to tubulin – a heterodimer protein

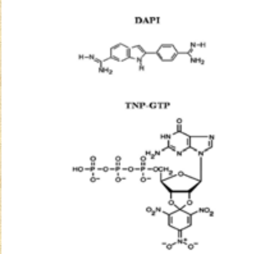

Figure 1. Structures of 4',6-diamidino-2-phenylindole (DAPI) and 2',3'-O-(2,4,6-trinitrocyclohexadienylidene)-GTP (TNP-GTP) at neutral or basic pH.

Assuming a κ^2 value of 2/3, one would calculate the DAPI-TNP-GTP distance to be ~43 Angstoms

But DAPI is bound non-covalently - hence has no local motion so its polarization is high (~0.48)

And, TNP-GTP is also non-covalently bound and has a short lifetime and hence a high polarization (~0.42)

These observed polarization values are close to the limiting polarization values for these probes: 93% and 100% respectively, for DAPI and TNP-GTP

Using the Dale-Eisenger-Blumberg plot one can then estimate that κ^2 can be anywhere between 0.02 and 3.7!

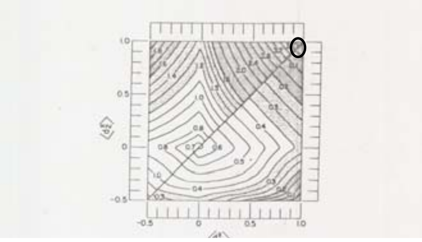

In fact the authors concluded, based on other information, that the distance between DAPI and TNP-GTP bound to tubulin was likely to ~ 30 Angstroms.

Determination of the efficiency of energy transfer (E)

$$E = \frac{k_T}{k_T + \sum_{i \neq T} k_i}$$

Where K_T is the rate of transfer and K_i is the rate for all other deactivation process

In the following discussion, we will consider only a single donor-acceptor distance and assume that the probes are precessing freely which will give a $\kappa^2 = 2/3$.

Determination of the efficiency of energy transfer (E)

Steady state method: Decrease in donor fluorescence. the fluorescence intensities of the donor is determined in absence and presence of the acceptor.

$$E = 1 - \frac{F_{da}}{F_d}$$

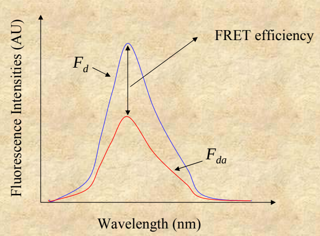

Determination of the efficiency of energy transfer (E)

Time-resolved method: decay of the donor fluorescence

If the fluorescence decay of the donor folowing pulse exitation is a single exponential then:

$$E = 1 - \frac{\tau_D}{\tau_D^0}$$

Where τ_D and τ_D^0 are the lifetime of the donor in presence and absence of acceptor, respectively

The distance dependence of the energy transfer efficiency (E)

$$r = \left(\frac{1}{E} - 1\right)^{1/6} R_0$$

Where r is the distance separating the donor and acceptor fluorophores, R_0 is the Förster distance.

Other equivalent form of this equation is found in the literature, among them:

$$E = R_0^6/(R_0^6 + r^6) \text{ or } E = 1/\left[1 + (r/R_0)^6\right]$$

The distance dependence of the energy transfer efficiency (E)

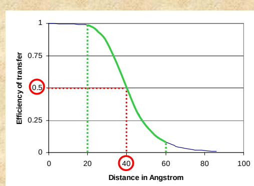

The efficiency of transfer varies with the inverse sixth power of the distance.

R_0 in this example was set to 40 Å. When the E is 50%, $R=R_0$

Distances can be measured between 0.5 R_0 and ~1.5R_0. Beyond these limits, we can often only say that the distance is smaller than 0.5 R_0 or greater than 1.5R_0. If accurate distance measurement is required then a probe pair with a different R_0 is necessary.

An elegant example of the use of FRET methodologies to study protein systems is given by the work of Lillo et al. ("Design and characterization of a multisite fluorescence energy-transfer system for protein folding studies: a steady-state and time-resolved study of yeast phosphoglycerate kinase" Biochemistry. 1997 Sep 16;36(37):11261-72 and "Real-time measurement of multiple intramolecular distances during protein folding reactions: a multisite stopped-flow fluorescence energy-transfer study of yeast phosphoglycerate kinase" Biochemistry. 1997 Sep 16;36(37):11273-81)

Site-directed mutagenesis was used to introduce pairs of cysteine residues in the protein at the positions shown

The pairs studied were:

135 – 290; 75 – 290

290 – 412; 412 – 202

135 – 412; 412 - 75

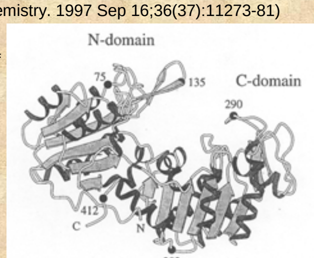

The donor was IAEDANS and the acceptor was IAF (iodoacetamindo-fluorescein). The various labeled protein products were separated by chromatography!

Table 1: Summary of the Labeled Proteins Examined for the Photophysical Characterization of Each Energy-Transfer Pair Cys$i$ → Cys$j$

sample	name	Cys$i$ → Cys$j$	no. of cysteines	fluorophore
donor only (D-PGK)	i-single cysteine	D- - -	1 (i)	AEDANS (i)
	j-single cysteine	- - -D	1 (j)	AEDANS (j)
	i-two cysteines	D- - -Cys	2 (i, j)	AEDANS (i)
	j-two cysteines	Cys- - -D	2 (i, j)	AEDANS (j)
	(i, j)-two cysteine average	D- - -Cys + Cys- - -D	2 (i, j)	AEDANS (i) + AEDANS (j)
	(i, j)-two cysteine "double donor"	D- - -D	2 (i, j)	AEDANS (i, j)
acceptor only	i-single cysteine	A- - -	1 (i)	AF (i)
	j-single cysteine	- - -A	1 (j)	AF (j)
donor-acceptor (D-PGK-A)	i, j specific label	D → A	2 (i, j)	AEDANS (i) and AF (j)
	j, i specific label	A ← D	2 (i, j)	AEDANS (j) and AF (i)
	i, j average label	D → A + A ← D	2 (i, j)	AEDANS (i) and AF (j) and + AEDANS (j) and AF (i)

Lifetime measurements were carried out on all samples

Table 5: Comparison of the Measured FRET Distances with That Predicted from the Crystal Structure[a]

energy-transfer pair	measured steady-state distance (Å)	measured time-resolved discrete distance R (Å)	χ^2	measured time-resolved distance distribution R_c (Å) [±2]	σ (Å)	χ^2	crystal structure $C_\alpha \to C_\alpha$ (Å)[a]	estimated dye-to-dye distances (Å)[b]
135 ↔ 290	43	43.3	2.7	39.4	7.3	1.3	39	39
		40.3[c]	1.6	38.8[c]	6.1	1.2		
135 ↔ 412	40	40.4	2.7	39.5	3.8	1.3	40	46
412 → 135	40	39.5	2.1	38.0	3.9	1.2		
		38.7	1.4	38.1[c]	3.4	1.3		
290 ↔ 412	69	63.6	1.4	64.8	13.5	1.3	48	56
		56.6[e]	1.8	58.6[e]	13.2	1.4		
75 ↔ 290	50	51.7	4.3	46.6	13.5	1.2	40	46
202 ↔ 412	39	41.7	1.5	37.8	6.6	1.1	26	34
412 → 75	47	48.2	3.1	44.8	13.5	1.4	32	46
all[d]	–	60–70	1.1	60–80	15–30	1.1	–	–

[a] Watson et al. (1982). [b] Donor-to-acceptor distance from MD simulations based on Watson et al. (1982) crystal structure. [c] Acceptor-side FRET measurements. [d] Unfolded samples (MOPS buffer at pH 7.5 and 25 °C and 2 M GuHCl). [e] MOPS buffer at pH 7.5 and 25 °C. D ↔ A: average labeled samples (donor distributed between the two Cys sites). D → A: specific labeled samples. Unless otherwise indicated, distance determinations are from donor-side experiments. The errors on the recovered distances are dominated by "nonfitting" sources and are estimated to be ±3 Å (see the text).

The intramolecular distances for the six energy transfer pairs are recovered for the each intermediate formed during the GuHCL induced unfolding of PGK

The authors proposed a specific structural transition associated with the unfolding of PGK from the native state (left) to the first unfolded state (right).

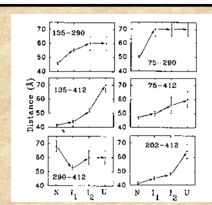

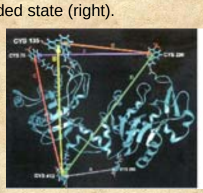

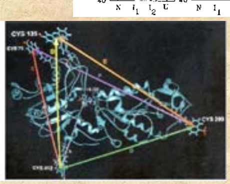

The C terminal domain (on the right of the monomer) is twisted by approximately 90º relative to the N-terminal domain resulting in an increase in the distances A,E and F and a shortening of the distance D. PM

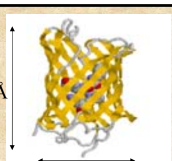

42Å

24Å

FRET experiments are often done *in vivo* using green fluorescent proteins (GFP)

GFP was originally isolated from the jellyfish *Aequorea victoria*. It is composed of 11 β-sheets, forming a barrel like structure called b-can, surrounding an a-helix containing the chromophore

The GFP is fused to the protein of interest and expressed in the organism under study.

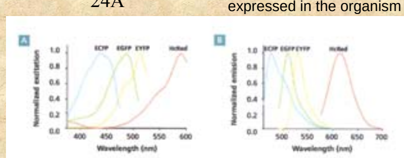

Figure 1. Excitation and emission spectra of BD Living Colors™ ECFP, EGFP, EYFP, and HcRed. HcRed's excitation maximum = 588 nm; emission maximum = 618 nm. EGFP's excitation maximum = 489 nm; emission maximum = 508 nm. EYFP's excitation maximum = 514 nm; emission maximum = 527 nm. ECFP's excitation maximum= 434 nm; emission maximum = 477 nm.

Mutations in the amino acids surrounding the chromophore results in GFP with different spectral properties.

Examples of the use of GFP and FRET *in vivo* can be found in: Tramier et al., 2003 "Homo-FRET versus hetero-FRET to probe homodimers in living cells" Methods Enzymol. 360:580-97

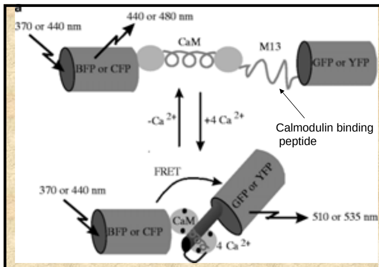

"Cameleon Proteins"

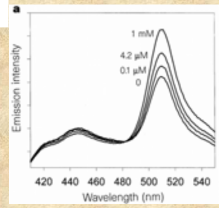

Fluorescent indicators for Ca2+based on green fluorescent proteins and calmodulin:
A. MIYAWAKI, J. LLOPIS, R. HEIM, J. M. MCCAFFERY, J. A. ADAMS, M. IKURA & R. TSIEN: *Nature (1997)* **388**, 882 - 887

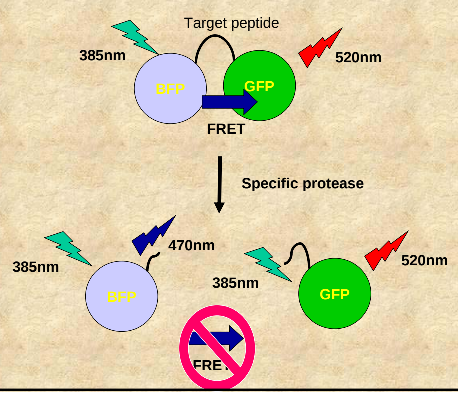

Homo-transfer of electronic excitation energy

So far, we considered the donor and acceptor molecules to be different. However, if the probe excitation spectrum overlaps its emission spectrum, FRET can occur between identical molecules.

« Il suffit qu'un transfert d'activation puisse se produire entre deux molécules voisines d'orientation différentes, c'est a dire portant des oscillateurs non parallèles, pour qu'il en résulte en moyenne une diminution de l'anisotropie de distribution des oscillateurs excites et par suite de la polarisation de la lumière émise. »
(F. Perrin *Ann de Phys.* 1929)

It suffices that a transfer of activation can occur between two neighboring molecules with different orientations, that is with non-parallel oscillators, in order to have, on average, a decrease in the anisotropy of the distribution of excited oscillators, and therefore a decrease of the polarization of the emitted light.

« …L'existence de transferts d'activation est expérimentalement prouvée pour de telles molécules par la décroissance de la polarisation de la lumière de fluorescence quand la concentration croit… »
(F. Perrin *Ann de Phys.* 1932)

…The existence of transfer of activation is proven experimentally for such molecules by the decrease in polarization of the fluorescent light when the concentration is increased…

Electronic energy transfer between identical fluorophores was originally observed by Gaviola and Pringsheim in 1924.

Über den Einfluß der Konzentration auf die Polarisation der Fluoreszenz von Farbstofflösungen.

Von **E. Gaviola** und **Peter Pringsheim** in Berlin.

Mit zwei Abbildungen. (Eingegangen am 24. März 1924.)

Tabelle 2. Uranin in ganz wasserfreiem Glycerin.

C	p	C	p	C	p	C	p
$\frac{1}{4}$	0	$\frac{1}{32}$	6,5	$\frac{1}{256}$	15	$\frac{1}{2048}$	39,2
$\frac{1}{8}$	?	$\frac{1}{64}$	8,1	$\frac{1}{512}$	19,5	$\frac{1}{4100}$	43,5
$\frac{1}{16}$	3,2	$\frac{1}{128}$	11,1	$\frac{1}{1024}$	30,7	etwa $\frac{1}{20000}$	45

(note: uranin is the sodium salt of fluorescein)

Homo-transfer of electronic excitation energy

"…Excitation transfer between alike molecules can occur in repeated steps. So the excitation may *migrate* from the absorbing molecule over a considerable number of other ones before deactivation occurs by fluorescence or other process. Though this kind of transfer cannot be recognized from fluorescence spectra, it may be observed by the decrease of fluorescence polarization…" (Förster, 1959)

A. B.

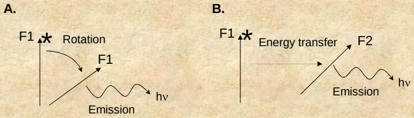

A. Depolarization resulting from rotational diffusion of the fluorophore. The excited fluorophore (F1*) rotates then emits light. **B.** The excited fluorophore (F1*) transfer energy to another fluorophore F2 which in turn emits light.

Weber's Red-Edge Effect

In 1960 Weber was the first to report that homotransfer among indole molecules disappeared upon excitation at the red-edge of the absorption band - this phenomenon is now known as the "Weber red-edge effect".

In 1970 Weber and Shinitzky published a more detailed examination of this phenomenon. They reported that in the many aromatic residues examined, transfer is much decreased or undetectable on excitation at the red edge of the absorption spectrum .

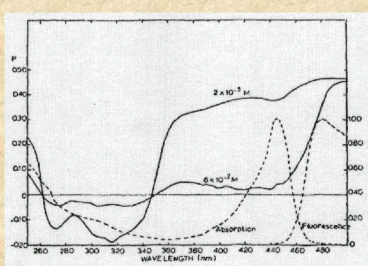

Distance determination using homotransfer

The efficiency of transfer can be calculated from a knowledge of the polarization in the absence and presence of energy transfer.

The steady state expression for the efficiency of energy transfer (E) as a function of the anisotropy is given by

$$E = 2(r_d - \langle r \rangle)/(r_d - r_a)$$

Where r_d and r_a are the anisotropy decay of the donor and acceptor only, respectively and $\langle r \rangle$ is the observed anisotropy in presence of both donor and acceptor. If κ^2 =2/3 then r_a = 0 and

$$E = 2(r_d - \langle r \rangle)/r_d$$

An example of homo-FRET used to study protein interactions is the work by Hamman et al (Biochemistry *35*:16680) on a prokaryotic ribosomal protein

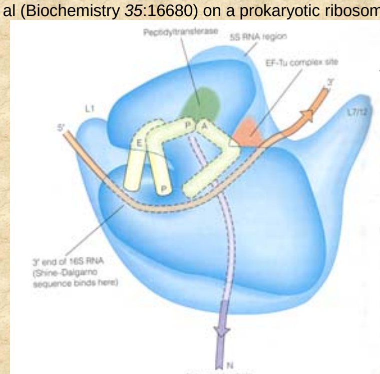

L7/L12 is present as two dimers in the ribosome. An X-ray structure of <u>monomeric</u> C-terminal domains led to the speculation that the C-terminal domains of L7/L12 interacted through hydrophobic surfaces as shown below

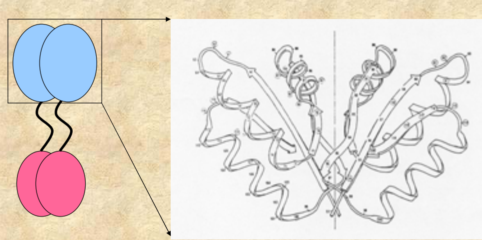

To study this protein fluorescence probes were introduced at specific locations along the L7/L12 peptide backbone.

To introduce these probes at specific locations site-directed mutagenesis was used to place cysteine residues in different locations

Sulfhydryl-reactive fluorescence probes were then covalently attached to these cysteine residues

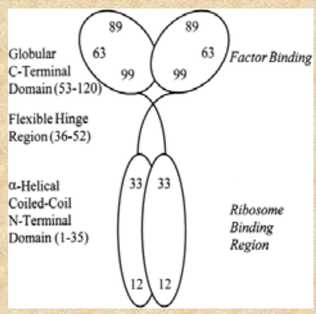

Subunit exchange experiments allowed the preparation of singly labeled dimers

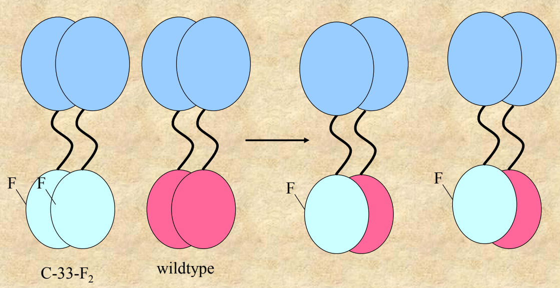

The presence of homoFRET was evident in the excitation polarization spectrum as shown by the Weber Red-Edge Effect.

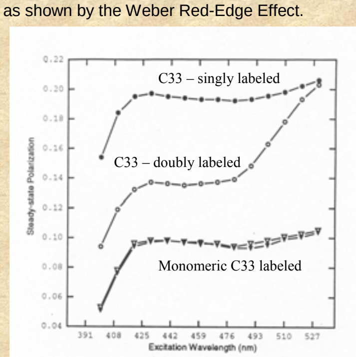

The polarization values, before and after subunit exchange, indicate which residues undergo homoFRET. The polarization data below are for fluorescein labeled constructs before (violet) and after (magenta) subunit exchange

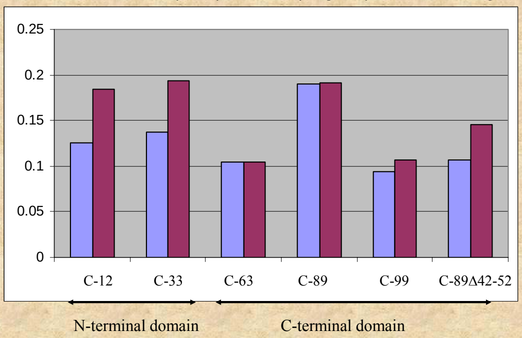

These changes in polarization due to homoFRET allow us to assign maximum proximity values for the C-terminal domains.

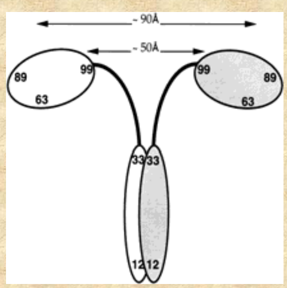

The conclusion is that the C-terminal domains are well-separated – contrary to the original model from the X-ray studies and the usual depictions in the literature

Homo-FRET Microscopy in Living Cells to Measure Monomer-Dimer Transition of GFP-Tagged Proteins

I. Gautier,* M. Tramier,* C. Durieux,* J. Coppey,* R. B. Pansu,† J-C. Nicolas,‡ K. Kemnitz,§ and M. Coppey-Moisan*

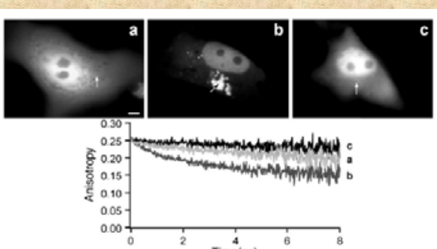

FIGURE 1 Subcellular fluorescence anisotropy decays of TK[illegible]GFP and TK[illegible]GFP proteins. (*Top*) Steady-state fluorescence images of Vero cells expressing TK[illegible]GFP (*a*) and TK[illegible]GFP (*b* and *c*). (*a* and *c*) Cells presenting only a diffuse cytoplasmic and nuclear fluorescence pattern. (*b*) Cells containing fluorescent aggregates. (*Bottom*) Time-resolved fluorescence depolarization from a cytoplasmic area of diffuse fluorescence (*a* and *c*) and from an area inside an aggregate (*b*). The subcellular location of the illuminated volume (~1 μm^3) from which the anisotropy decay was performed is indicated by an arrow. For cells containing aggregates, anisotropy decays from nuclear or cytoplasmic area of diffuse fluorescence were similar to that obtained from aggregates (*b*). Bar in *a*, 5 μm.

Biophys J, June 2001, p. 3000-3008, Vol. 80, No. 6

Quenching

A number of processes can lead to a reduction in fluorescence intensity, i.e., quenching

These processes can occur during the excited state lifetime – for example collisional quenching, energy transfer, charge transfer reactions or photochemistry – or they may occur due to formation of complexes in the ground state

We shall focus our attention on the two quenching processes usually encountered – namely collisional (dynamic) quenching and static (complex formation) quenching

Collisional Quenching

Collisional quenching occurs when the excited fluorophore experiences contact with an atom or molecule that can facilitate non-radiative transitions to the ground state. Common quenchers include O_2, I^-, Cs^+ and acrylamide.

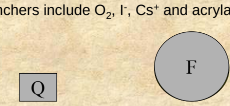

In the simplest case of collisional quenching, the following relation, called the **Stern-Volmer equation**, holds:

$$F_0/F = 1 + K_{SV}[Q]$$

where F_0 and F are the fluorescence intensities observed in the absence and presence, respectively, of quencher, [Q] is the quencher concentration and K_{SV} is the **Stern-Volmer quenching constant**

In the simplest case, then, a plot of F0/F versus [Q] should yield a straight line with a slope equal to K_{SV}.

Such a plot, known as a Stern-Volmer plot, is shown below for the case of fluorescein quenched by iodide ion (I^-).

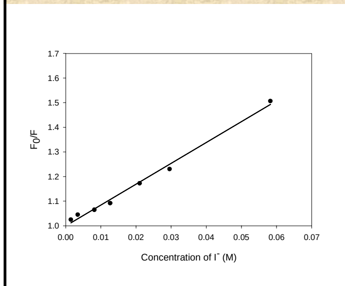

In this case, K_{SV} ~ 8 L-mol^{-1}

$K_{SV} = k_q \tau_0$ where **k_q is the bimolecular quenching rate constant** (proportional to the sum of the diffusion coefficients for fluorophore and quencher) and **τ_0 is the excited state lifetime** in the absence of quencher.

In the case of purely collisional quenching, also known as ***dynamic*** quenching,:

$$F_0/F = \tau_0/\tau.$$

Hence in this case: $\tau_0/\tau = 1 + k_q \tau[Q]$

In the fluorescein/iodide system, τ = 4ns and k_q ~ 2 x 10^9 M^{-1} sec^{-1}

Static Quenching

In some cases, the fluorophore can form a stable complex with another molecule. If this *ground-state* is non-fluorescent then we say that the fluorophore has been statically quenched.

In such a case, the dependence of the fluorescence as a function of the quencher concentration follows the relation:

$$F0/F = 1 + Ka[Q]$$

where Ka is the association constant of the complex. Such cases of quenching via complex formation were first described by Gregorio Weber.

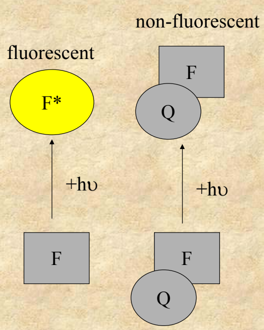

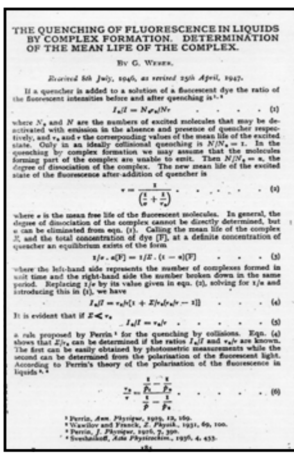

THE QUENCHING OF FLUORESCENCE IN LIQUIDS BY COMPLEX FORMATION. DETERMINATION OF THE MEAN LIFE OF THE COMPLEX.

By G. Weber.

Received 8th July, 1946, as revised 25th April, 1947.

If a quencher is added to a solution of a fluorescent dye the ratio of the fluorescent intensities before and after quenching is[1,2]

$$I_0/I = N_0\tau_0/N\tau \quad (1)$$

where N_0 and N are the numbers of excited molecules that may be de-activated with emission in the absence and presence of quencher respectively, and τ_0 and τ the corresponding values of the mean life of the excited state. Only in an ideally collisional quenching is $N/N_0 = 1$. In the quenching by complex formation we may assume that the molecules forming part of the complex are unable to emit. Then $N/N_0 = \alpha$, the degree of dissociation of the complex. The new mean life of the excited state of the fluorescence after addition of quencher is

$$\tau = \frac{1}{\left(\frac{1}{\sigma} + \frac{1}{\tau_0}\right)} \quad (2)$$

where σ is the mean free life of the fluorescent molecules. In general, the degree of dissociation of the complex cannot be directly determined, but α can be eliminated from eqn. (1). Calling the mean life of the complex Σ, and the total concentration of dye [F], at a definite concentration of quencher an equilibrium exists of the form

$$1/\sigma \cdot \alpha[F] = 1/\Sigma \cdot (1 - \alpha)[F] \quad (3)$$

where the left-hand side represents the number of complexes formed in unit time and the right-hand side the number broken down in the same period. Replacing $1/\sigma$ by its value given in eqn. (2), solving for $1/\alpha$ and introducing this in (1), we have

$$I_0/I = \tau_0/\tau[1 + \Sigma/\tau_0(\tau_0/\tau - 1)] \quad (4)$$

It is evident that if $\Sigma \ll \tau_0$

$$I_0/I = \tau_0/\tau \quad (5)$$

a rule proposed by Perrin[1] for the quenching by collisions. Eqn. (4) shows that Σ/τ_0 can be determined if the ratios I_0/I and τ_0/τ are known. The first can be easily obtained by photometric measurements while the second can be determined from the polarisation of the fluorescent light. According to Perrin's theory of the polarisation of the fluorescence in liquids[3,4]

$$\frac{\tau_0}{\tau} = \frac{\frac{1}{p_0} - \frac{1}{p_0}}{\frac{1}{p} - \frac{1}{p_0}} \quad (6)$$

[1] Perrin, *Ann. Physique*, 1929, 12, 169.
[2] Wawilov and Franck, *Z. Physik.*, 1931, 69, 100.
[3] Perrin, *J. Physique*, 1926, 7, 390.
[4] Svesnikoff, *Acta Physicochim.*, 1936, 4, 453.

Weber studied the quenching of several fluorophores by iodide as well as aromatic molecules. He observed the polarization and hence indirectly observed the lifetime of the fluorophore.

In the case of static quenching the lifetime of the sample will not be reduced since those fluorophores which are not complexed – and hence are able to emit after excitation – will have normal excited state properties. The fluorescence of the sample is reduced since the quencher is essentially reducing the number of fluorophores which can emit.

Below is shown his original plot for riboflavine quenching by iodide and by hydroquinone – note that he plots 1/p versus I/I_0

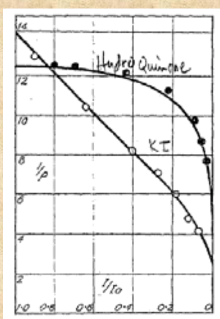

FIG. 2.

Note how the polarization increases rapidly upon addition of iodide – due to the decrease in the excited state lifetime via collisional (dynamic) quenching

In the case of hydroquinone, initially the intensity decreases with no significant change in the polarization – hence the lifetime is not decreasing. Only at higher concentrations of hydroquinone do we see evidence for dynamic quenching.

If both static and dynamic quenching are occurring in the sample then the following relation holds:

$$F_0/F = (1 + k_q \tau[Q])(1 + K_a[Q])$$

In such a case then a plot of F_0/F versus [Q] will give an upward curving plot

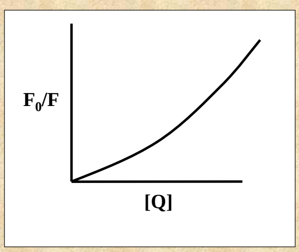

The upward curvature occurs because of the $[Q]^2$ term in the equation

However, since the lifetime is unaffected by the presence of quencher in cases of pure static quenching, a plot of τ_0/τ versus [Q] would give a straight line

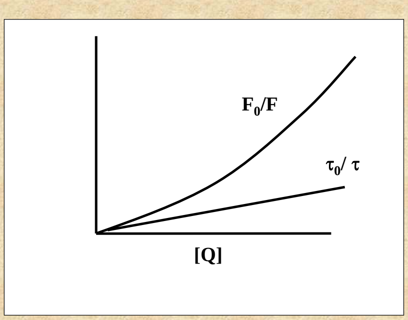

An elegant early study of dynamic and static quenching was carried out by Spencer and Weber ((1972) "Thermodynamics and kinetics of the intramolecular complex in flavin adenine dinucleotide". In *Structure and Function of Oxidation Reduction Enzymes*, A. Akeson and A. Ehrenberg (eds.), Pergamon, Oxford-New York, pp. 393-399.

THE INTRAMOLECULAR COMPLEX IN FAD 397

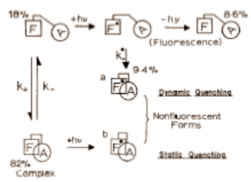

FIG. 4. Kinetic scheme for the intramolecular quenching of FAD in water. The excited state complexes, *a* and *b*, may be identical.

Sometimes you will see the equation for simultaneous static and dynamic quenching given as:

$$F_0/F = (1 + K_{SV}[Q])\mathbf{e}^{\mathbf{V[Q]}}$$

where the term $\mathbf{e}^{\mathbf{V[Q]}}$ is used as a phenomological descriptor of the quenching process. The term V in this equation represents an *active volume* element around the fluorophore such that any quencher within this volume at the time of fluorophore excitation is able to quench the excited fluorophore.

Non-linear Stern-Volmer plots can also occur in the case of purely collisional quenching if some of the fluorophores are less accessible than others. Consider the case of multiple tryptophan residues in a protein – one can easily imagine that some of these residues would be more accessible to quenchers in the solvent than other.

In the extreme case, a Stern-Volmer plot for a system having accessible and inaccessible fluorophores could look like this:

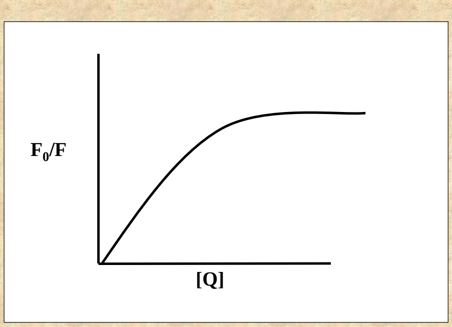

The quenching of LADH intrinsic protein fluorescence by iodide gives, in fact, just such a plot. LADH is a dimer with 2 tryptophan residues per identical monomer. One residue is buried in the protein interior and is relatively inaccessible to iodide while the other tryptophan residue is on the protein's surface and is more accessible.

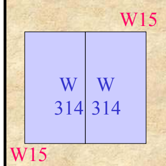

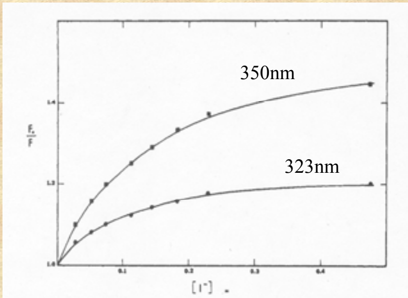

In this case (from Eftink and Selvidge, Biochemistry 1982, 21:117) the different emission wavelengths preferentially weigh the buried (323nm) or solvent exposed (350nm) trytptophan.

Acrylamide quenching of single tryptophan proteins.
K_q is reflected in in λ_{max}

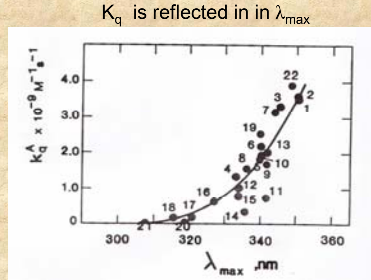

From Eftink, 1991

Quenching may be affected by the charge on the fluorophore and quencher